JOURNAL OF AIRCRAFT
Vol. 29, No. 6, Nov.–Dec. 1992

Buffet Excitation of Wings at Low Speeds

Steven J. Zan*
Institute for Aerospace Research, Ottawa K1A 0R6, Canada
and
David J. Maull†
Cambridge University, Cambridge CB2 1PZ, England, United Kingdom

Wind-tunnel experiments were undertaken to investigate the unsteady excitation arising from separated flow at low speeds. A series of untapered wing models with a common section chosen to be insensitive to Reynolds number effects was used in the investigation. The models had sweep angles of −20, 0, and 30 deg, and aspect ratios ranging from 6 to 16. The excitation was measured indirectly using wing-root strain gauges and presented in terms of the buffet excitation parameter. The experimental data obtained in this investigation indicate that this parameter attains a common limit under poststall conditions irrespective of wing planform; physical reasons for the limit are discussed. Poststall conditions refer to angles of attack in excess of that at which the lift is maximized. Buffet excitation can attain larger values at lower incidences, and also at high incidences for lower reduced frequencies, which correspond more closely to rigid-body modes.

Nomenclature

AR	=	aspect ratio
b	=	tip-to-tip wing span
C_R	=	root bending-moment coefficient
c	=	wing chord
c_L	=	sectional life coefficient
$F(n)$	=	Theodorsen function
f	=	frequency, Hz
f_0	=	modal frequency
$G(n)$	=	dimensionless spectral density of excitation
m	=	mode generalized mass
n	=	reduced frequency, fc/V
$\sqrt{nG(n)}$	=	buffet excitation parameter
q	=	dynamic pressure
RBM	=	time-averaged root bending moment
S	=	wing area
V	=	freestream velocity
y	=	spanwise coordinate
α	=	angle of incidence
ζ	=	total modal damping
η	=	$2y/b$
Λ	=	sweep angle
ρ	=	air density
σ	=	modal rms wing-tip acceleration
ϕ	=	measured mode shape

Introduction

UNSTEADY aerodynamic loads induced by flow separations can cause aircraft dynamic responses. These responses are structural deformations at reduced frequencies of order 0.3, and rigid-body motions at reduced frequencies an order of magnitude lower. This article focuses on such structural deformations that are referred to as buffeting. The excitation arising from the separated flow that causes the structural deformations is referred to as buffet.[1]

Buffet excitation generally becomes significant near the incidence at which there is a deviation from linearity of the lift-curve slope. Further increase in incidence will generally increase the buffeting. Based on a limited number of flight-test and wind-tunnel observations, it has been suggested that as an aircraft reaches a handling boundary, the buffet excitation remains bounded and of the same magnitude, irrespective of wing planform and separation development.[2] This excitation is quantitatively described using the buffet excitation parameter, $\sqrt{nG(n)}$, in the notation of Ref. 1 where

$$\sqrt{nG(n)} = (2m\sigma\sqrt{\zeta})/\sqrt{\pi}qS) \tag{1}$$

The reasons for, and further confirmation of the bounded excitation (referred to as the heavy buffet limit) have been suggested as useful topics for further research.[2]

For an investigation of aircraft dynamic response to separated flow, it is common practice to measure the aerodynamic excitation and/or the aircraft response, although it is also prudent to consider the structure of the surrounding flowfield. Structures found in separated flow over aircraft wings at low speeds include bubbles, foci of separation, tip vortices, and three-dimensional spanwise cells. Researchers have associated buffet excitation with each of these structures.

The presence of three-dimensional cells on a wing upper surface has been reported based on flow visualization of slightly stalled airfoils.[3,4] For a wing that developed a trailing-edge separation,[3] the "cells" were seen to grow towards the leading edge with increasing incidence. A definite increase in buffeting was reported when the separation line reached the leading edge, although any qualitative or quantitative description of this buffeting is lacking.

Foci of separation are discussed in detail in Ref. 5, where it is stated that the buffet phenomenon on swept wings is thought to be related to the unsteady characteristics of foci. However, in Ref. 6, flow visualization techniques were used to establish the presence of foci of separation on a stalled swept wing in a detailed buffet investigation, yet no relationship between foci of separation and buffet was found in this work, which appears to contradict the statement in Ref. 5.

Separation bubbles have been the subject of many investigations. In particular, considerable experimental evidence has been amassed on the self-similarity of various static and dynamic properties of separation bubbles.[7] The influence of leading-edge, snag, and tip vortices on buffet and buffeting is discussed in Ref. 8.

The primary focus of this research was to experimentally investigate the buffet excitation parameter for a series of sharp leading-edge wing models in a low-speed flow over a range

Received July 27, 1991; revision received Dec. 9, 1991; accepted for publication Dec. 9, 1991. Copyright © 1991 by National Research Council of Canada. Published by the American Institute of Aeronautics and Astronautics, Inc., with permission.

*Research Officer, Applied Aerodynamics Laboratory.
†Reader, Engineering Department.

of incidence from 0–40 deg. The analysis was primarily confined to the fundamental bending mode, although a limited number of results were obtained for the second (overtone) bending mode. In particular, it was of interest to determine whether the magnitude of the buffet excitation parameter remained bounded as had been suggested, and if so, to uncover physical reasons for this result.

The work reported herein, although based on the doctoral thesis of the first author,[9] contains additional experimental observations and discussion.

Description Of Experiments

The experiments were conducted in the University of Cambridge low-speed wind tunnel that has a test section cross section of 1.2 × 1.7 m and a maximum speed of 60 m/s. The Reynolds numbers obtained in the experiment were low, only 0.1×10^6–0.5×10^6 based on wing chord (76 mm).

The behavior of 17 untapered wing models was investigated,[9] although not all models are discussed here. The models were stiff but not rigid, and were cantilevered out from the wind-tunnel floor in a "half-model" configuration. A simulated fuselage was not incorporated. Fundamental bending mode accelerations were determined by means of a full-bridge wing-root strain gauge. The bridge had been calibrated prior to testing by exciting the model in that mode and relating the output to a wing-tip-mounted accelerometer. Aspect ratios ranged from 6 to 16 with three sweep angles −20, 0, and 30 deg. Each model was tested over a range of incidence from 0 to 40 deg in 2 deg increments at three wind speeds, and therefore, three reduced frequencies.

In Ref. 10 it is argued that $G(n)$ is a function of Mach and Reynolds numbers, wing geometry, and angle of attack. By using the wing section shown in Fig. 1 (which has a sharp leading edge) the effect of Reynolds number was minimized. Furthermore, there is evidence to suggest that once the flow has fully separated from an aircraft wing, the unsteady pressures acting on the wing are insensitive to Reynolds number effects.[11] Also, compressibility effects are considered insignificant in this investigation as the Mach number did not exceed 0.2. Thus, for this investigation, $G(n)$ is a function only of wing geometry and angle of attack.

Knowledge of the mean flow characteristics and of the mean aerodynamic loads, was a prerequisite to understanding the unsteady flows and dynamic loads, which were of primary interest in this investigation. The mean aerodynamic loads acting on the wing models were measured using the wing-root strain gauges and converted to a nondimensional coefficient C_R defined as

$$C_R = \mathrm{RBM}/qS(b/2) \tag{2}$$

As an aid to understanding the mean flow characteristics, surface oil-flow visualization experiments were undertaken to determine the skin-friction lines.

Complete details of the experimental procedure may be found in Ref. 9. Approximately 1600 cycles of wing motion (fundamental mode) were recorded for each combination of incidence, wing model, and velocity. The sampling rate was about 20 times that of the fundamental bending mode frequency in all cases. These sampling conditions ensured convergence of the root-mean-square (rms) value of the signal and yielded damping estimates with a standard deviation of approximately 15% (95% confidence level) using the Randomdec technique.[12] In most cases this damping was predominantly structural in origin, however, in some cases appreciable aerodynamic damping was present. Later in this article, some quantitative assessments are made regarding the level of aerodynamic damping in separated flow for two of the wing models used in this investigation.

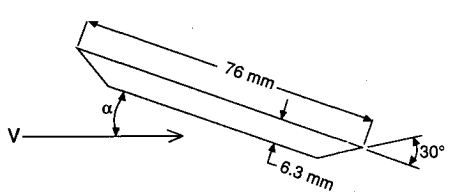

Fig. 1 Wing section.

Unswept Wing Models

Figure 2 presents the values of C_R as a function of incidence for the unswept wing models. Surface oil-flow visualization experiments performed on these models established that the leading-edge separation bubble, which formed over the upper surface for a small positive incidence, would fail to reattach for incidences greater than about 4.5 deg. The slope of the mean root bending-moment coefficient is seen to decrease at about 4.5 deg incidence, although, up to an incidence of 10 deg or so, the actual coefficient continues to rise. For the unswept wing models, this latter incidence will be referred to as the stall angle. Now in Ref. 13, measurements of lift on a two-dimensional double-wedge plate spanning a wind tunnel are reported where it is stated that a leading-edge separation bubble may enhance the magnitude of lift (provided that the bubble reattaches to the upper surface). Thus, in this experiment the increase in C_R over the range 5 deg $< \alpha <$ 10 deg cannot be attributed to the bubble that is present on the upper surface and now closes in the wake. The continued increase in normal force and, therefore, root bending moment beyond 4.5 deg incidence, must be due to the attached flow resulting from the wing tip vortex (indicated in Fig. 3 at 10 deg incidence).

Oil flow visualization experiments performed at a Reynolds number of 200,000 revealed similar skin-friction lines on the suction surfaces for the various unswept wing models. Models with aspect ratios of 6, 8, and 16 were used for the flow visualization investigation. The surface streamlines are shown schematically in Fig. 3 for four incidences, and are presented for a spanwise distance of three chords, inboard from the tip. For a model with an aspect ratio greater than six, the flow pattern inboard of what is presented, can be inferred from the skin-friction line characteristics near the right edge of each figure. However, in all cases, the skin-friction lines within one chord of the wing root showed evidence of the vortex which forms at the wing root/wind tunnel wall junction. Wing-root flows were not of interest here because they contribute little to the static or dynamic root bending moments.

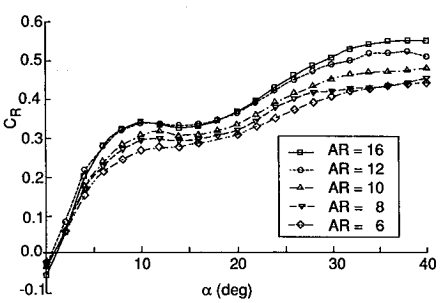

Fig. 2 Variation in mean root bending moment coefficient with incidence Λ = 0 deg.

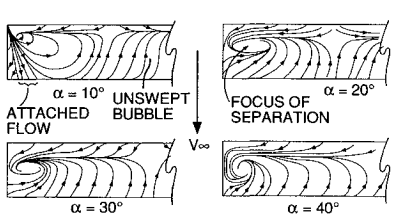

Fig. 3 Skin-friction lines—unswept wing models.

The flow above the wing, and away from the tip or root, can be characterized by a large unswept separation bubble with several recirculation bubbles contained therein. For a low-speed flow like that present in this investigation, the dynamic loading is produced by large-scale instabilities and movements in the separated shear-layer feeding through the bubble onto the wing surface, rather than from local small-scale fluctuations.

There is a region of attached flow near the wing tip at 10 deg incidence that is not evident at the higher incidences in Fig. 3, suggesting that the core of the wing tip vortex is lifting off the wing surface at an incidence in excess of 10 deg. At these higher incidences, and within about one chord of the wing tip, is a focus of separation. Smoke flow visualization established that the fluid entrained by the focus would lift from the surface, roll up into a vortex and be convected downstream, combining with the wake. It also suggested that the orientation of this vortex relative to the wing model was not fixed, but rather tended to wobble. Although the relative sizes of these regions shown are intended to be accurate, the precise bounds of a focus are difficult to establish.

Figure 4 presents the variation in buffet excitation parameter with incidence for the aspect-ratio-eight unswept steel wing model. The buffet excitation parameter takes on nonzero values for all positive incidences because separated flow is present on the upper (and lower) surface for these incidences. The buffet excitation parameter increases with incidence up to an incidence of about 10 deg, at which C_R is also at a local maximum (Fig. 2). $\sqrt{nG(n)}$ attains a value of about 0.006 at this incidence, that is twice that of the heavy buffet limit. According to Ref. 14, this severe level of buffeting in a low-speed flow should arise from either a bistable separation or some kind of aerodynamic resonance. However, as discussed in Ref. 9, smoke flow visualization indicated the tip vortex was not stationary, but tended to move about above the wing model. It was concluded (but not confirmed) that the most probable source of the severe buffet excitation is movement of the tip vortex, since this would lead to substantial pressure changes at the wing tip which increase the excitation and, therefore, the magnitude of $\sqrt{nG(n)}$. Buffet excitation resulting from wing-tip vortices was reported in Ref. 8; although no direct connection can be made between the two investigations as the relevant reduced frequencies for that investigation were an order of magnitude greater than the values with which this article is concerned.

As incidence is increased beyond that at which $C_{R\max}$ occurs, the value of $\sqrt{nG(n)}$ decreases and then becomes essentially constant at about 0.003 (which corresponds to the heavy buffet limit). At high incidences, $\sqrt{nG(n)}$ decreases slightly with increasing values of reduced frequency. The tip vortex does not influence the aerodynamic loading at these high incidences, so it can be said that for this case the excitation arises from the unswept bubble on the upper surface. Based on experimental evidence, it was suggested in Ref. 9 that excitation arising from the focus of separation is significant at much lower values of reduced frequency, and thus not contributing to the excitation here.

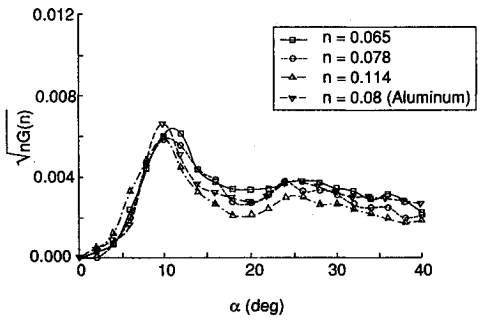

Fig. 4 Variation in $\sqrt{nG(n)}$ with incidence AR = 8, Λ = 0 deg.

For a wind-tunnel investigation in which there is a degree of flexibility in the model, there arises the possibility that the motion of the model will affect the unsteady flowfield surrounding the wing. Additionally, concerns about static aeroelastic distortion arise when the model is flexible. However, in Ref. 9, it was shown that static aeroelastic distortion was not a significant factor in this investigation. To assess the sensitivity of the buffet excitation parameter to model motion amplitude, unswept wing models with aspect ratios of 8 and 16 were constructed of aluminum, but were otherwise identical to their steel counterparts. Analysis of the wind-tunnel test results showed that the wing-tip deflections for the aluminum models were about three times those of the steel wing models.

The effect of the increased flexibility on the buffet excitation parameter was negligible for the aspect-ratio-eight wing models as indicated in Fig. 4. It can be concluded that under these conditions the model motion does not interfere or interact with the loads arising from the separated flow and these loads can be considered motion-independent. At most, the model motion may result in an aerodynamic damping term, the magnitude of which (when expressed as a percent of the critical value) would be larger for the aluminum model.

In Figs. 5a and 5b, values of $\sqrt{nG(n)}$ obtained from each of the unswept wing models, are plotted against reduced frequency for two angles of incidence, one corresponding to stall (α = 10 deg) and one well beyond stall (α = 30 deg). Results from a specific wing model are connected by a solid line and the particular aspect ratio is indicated. Values of the buffet excitation parameter as a function of incidence for each of the unswept wing models have been reported elsewhere.[15] Computation of $G(n)$ at 10 deg incidence revealed self-similar "flat" spectra for all wing models.[9] Thus, as the aspect ratio increases, $\sqrt{nG(n)}$ will decrease as indicated in the figure.

The heavy buffet limit of 0.003 is again evident at the higher incidence and at reduced frequencies characteristic of low-speed flight. Severe levels of excitation are present for reduced frequencies corresponding to rigid-body modes at these large angles of incidence, and these levels are associated with the presence of a focus of separation. From the point of view of buffet, this excitation is of little interest; however, this magnitude of excitation may be of some concern with respect to the rigid-body dynamics of an aircraft, expecially in the roll mode.

Digital spectral analysis of the wing-root strain-gauge time histories revealed that in a limited number of cases a distinct response peak occurred at the second (overtone) bending mode frequency. This response was analyzed for the unswept aspect-ratio-sixteen wing models at 10, 20, 30, and 40 deg of incidence. Computation of $\sqrt{nG(n)}$ from the response in this

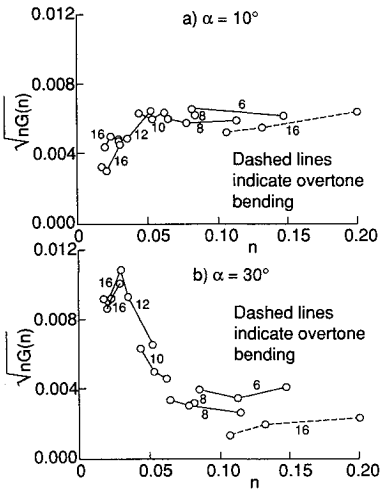

Fig. 5 Influence of reduced frequency on $\sqrt{nG(n)}$, Λ = 0 deg.

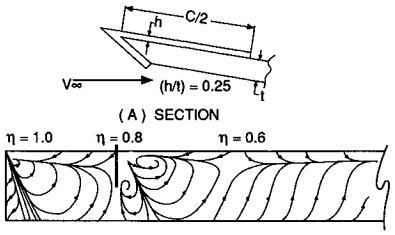

Fig. 6 Vestigal fence.

mode was not as straightforward as for the fundamental bending mode. The evaluation of the generalized mass in the second mode proved to be experimentally difficult, and so the value determined analytically from beam vibration theory was used. Similarly, it proved difficult to calibrate the strain-gauge bridge as a function of wing-tip acceleration in the second mode. Recourse was made to determine a value using an analytical method based on the theoretical mode shape, measured natural frequency, and known strain-gauge gauge factor. (For the first bending mode, a comparison of the experimental calibration with the result obtained using this analytical method for that mode, revealed good agreement.) The total damping in the second mode was determined using the half-power point method, and as such there is greater uncertainty in the damping estimates for this mode than for the fundamental mode damping estimates obtained by way of the Randomdec method.

Figures 5a and 5b show that the value of the buffet excitation parameter for the overtone bending mode is in reasonable agreement with the values obtained in the first mode at similar values of reduced frequency but at a lower aspect ratio. The result should not be surprising, as one would only expect modal effects to exist if there are significant motion-dependent aerodynamic loads in-phase with the displacement of the wing. Such effects are not likely to be found in a low-speed flow at these reduced frequencies.

The effect of a small fence on buffet excitation was studied by mounting a small fence at $\eta = 0.8$ on the aspect-ratio-sixteen wing model as shown in Fig. 6. While the fence altered the mean skin-friction lines considerably at 10 deg incidence (no appreciable change in skin-friction pattern was observed at 20, 30, or 40 deg incidence), the values of the buffet excitation parameter remained unchanged over the entire incidence range. Thus, the excitation must arise from the shear-layer instabilities near the top of the bubble, rather than from local unsteady pressures and velocities near the suction surface. It should be noted, that the reduced frequency range over which the experiments with this fence were conducted, was $0.017 \leq n \leq 0.030$, far below values expected for buffeting in low-speed flight.

Aft-Swept Wing Models

Figure 7 is a plot of the mean root bending-moment coefficients as a function of incidence for the aft-swept wing models. For incidences greater than those at which the separation bubble failed to reattach on the unswept wing models (about 4.5 deg), these coefficients are reduced compared to those of the unswept wing models. Surface oil-flow visualization established that attached flow arising from a tip vortex did not exist for the swept wing models for any incidence greater than 2.5 deg, presumably because of the local tip geometry. Thus, when the leading-edge separation bubble reached the trailing edge on the aft-swept wing models, there was no further contribution to lift, and so the mean root bending-moment coefficients do not increase appreciably with a further increase in incidence up to 15 deg. As will be shown, there is a significant change in the buffet excitation over this incidence range. Beyond about 15 deg of incidence, C_R increased again.

The results of the oil flow experiments performed on the aft-swept wing models indicated that the upper surface is dominated by a swept separation bubble at all incidences (Figs. 8 and 9). In Fig. 8 evidence of a small focus of separation near

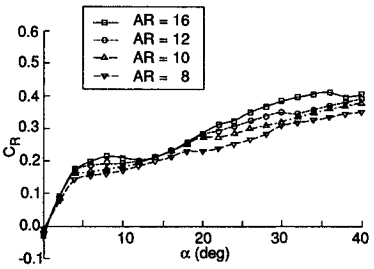

Fig. 7 Variation in mean root bending moment coefficient with incidence Λ = 30 deg.

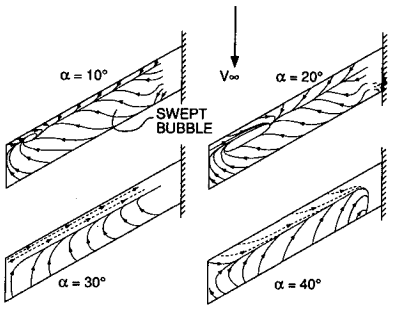

Fig. 8 Skin-friction lines—AR = 8, Λ = 30 deg.

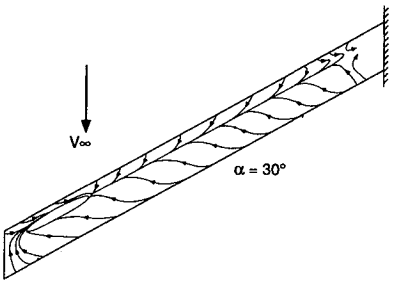

Fig. 9 Skin-friction lines—AR = 16, Λ = 30 deg.

the outboard edge, similar to that found on the unswept wing models, can be seen clearly at 10 and 20 deg of incidence, but is not found at higher incidences. At the two highest incidences in Fig. 8, dashed skin-friction lines are indicative of low shear stress.

The surface streamlines for the aft-swept aspect-ratio-twelve and -sixteen wing models were in general agreement with those of the aspect-ratio-eight wing model at incidences of 10 and 20 deg, the midspan flow simply occurring over a larger area. However, at 30 deg incidence and beyond (Fig. 9) the pattern was unlike those for the aspect-ratio-eight aft-swept wing model. In these cases, the flow pattern was similar to those at lower incidences with a focus of separation near the wing tip. This change in the mean flow pattern possibly arises because the higher aspect-ratio wing models have greater circulation outboard, consequentially reversing the direction of the spanwise pressure gradient.

The influence of aft sweep on the buffet excitation parameter for an aspect-ratio-eight wing model is shown in Fig. 10 wherein the results for the aspect-ratio-eight unswept steel wing model at $n = 0.08$ are also included. Over the incidence range 8 deg $< \alpha <$ 16 deg, the value of $\sqrt{nG(n)}$ is considerably reduced for the wing model with sweep. Considering the fact that flow visualization did not establish the presence of a tip vortex on the upper surface of the aft-swept wing models for any incidence greater than 2.5 deg, it now seems quite probable that the tip vortex is responsible for the increased buffet excitation of the unswept wing models over this incidence range. However, this conjecture cannot be confirmed in the absence of detailed unsteady pressure measurements near the wing tip. At higher incidences, the effect of 30 deg sweep on

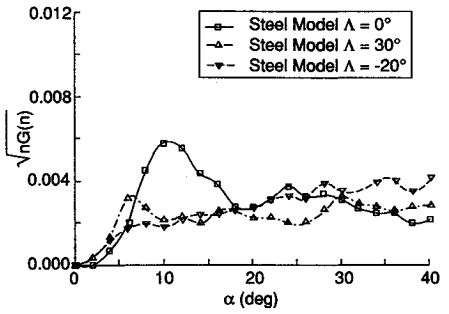

Fig. 10 Variation in $\sqrt{nG(n)}$ with incidence for three sweep angles, AR = 8.

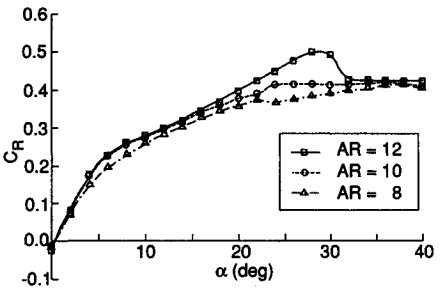

Fig. 11 Variation in mean root bending moment coefficient with incidence Λ = −20 deg.

the buffet excitation parameter is minimal. This is an important point because this combination of aspect ratio and reduced frequencies is representative of those commonly occurring for subsonic aircraft in flight. It is also noteworthy that the value of $\sqrt{nG(n)}$ corresponds well with the heavy buffet limit of 0.003. For all incidences, the swept wing model flow is dominated by a swept bubble and it can be concluded that the unsteady pressures associated with this bubble are responsible for the buffet excitation. At high incidences, flow over the unswept wings is also dominated by a separation bubble (in this case unswept), and in both cases the integrated effect of the excitation is to produce the same value of $\sqrt{nG(n)}$. Experimental evidence suggests that the focus of separation which exists at large angles of incidence, for the aft-swept wing models with larger aspect ratios, is again associated with excitation at reduced frequencies corresponding to rigid-body modes, as discussed in Ref. 9.

Forward-Swept Wing Models

For a forward-swept wing, stall occurs initially at the root, and progresses in a spanwise manner towards the tip, the outcome of which is a more gradual variation in C_R with incidence as is shown in Fig. 11. The shape of the curve for the aspect-ratio-twelve wing model suggests that attached flow and therefore, high suction, exists at the wing tip up to approximately 30 deg incidence.

Flow visualization experiments established that the separated flow is again dominated by a swept bubble. Additionally, for the forward-swept wing models, a vortex originated at the apex of the wing, as shown in Fig. 12 for the aspect-ratio-eight wing model. As incidence increases, the region of attached flow resulting from the presence of the vortex near the wing tip decreases in size, and at an incidence of 30 deg the tip vortex no longer produced attached flow on the surface. In contrast, the top vortex continued to strongly influence the tip flow for the forward-swept aspect-ratio-twelve wing model at 30 deg (Fig. 13), but not at 32 deg, possibly because the vortex had lifted off. Smoke flow visualization at 30 deg incidence established that the tip vortex moved about in an irregular fashion at this incidence. The tip vortex is evidently responsible for the high suctions and increased value of C_R for the aspect-ratio-twelve wing model at 30 deg.

Considering the manner by which flow separation progresses with increasing incidence on forward swept wings, it would be expected that for appropriate incidences (low α) the magnitude of the buffet excitation parameter would be less for a forward-swept wing than for an unswept wing, simply because the separated flow region is nearer to the wing root. This is shown to be the case in Fig. 10 for the aspect-ratio-eight forward-swept wing model. At 10 deg incidence the level of $\sqrt{nG(n)}$ is less by a factor of three for the forward-swept wing model, than for the unswept wing model, despite the fact that a tip vortex is present in both cases. It is thought that away from the incidence at which $C_{R\max}$ occurs, the tip vortex must remain relatively stationary, and therefore not contribute to buffet excitation for the forward-swept wing model.

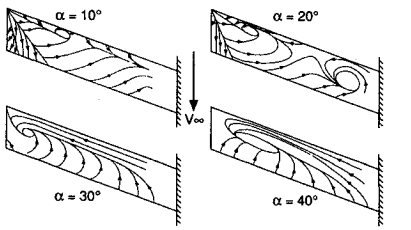

Fig. 12 Skin-friction lines—AR = 8, Λ = −20 deg.

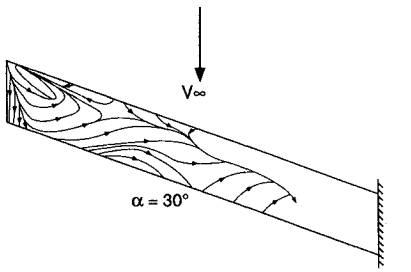

Fig. 13 Skin-friction lines—AR = 12, Λ = −20 deg.

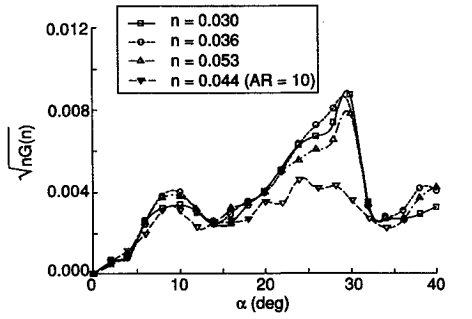

Fig. 14 Variation in $\sqrt{nG(n)}$ with incidence Λ = −20 deg.

In light of the discussion of the effects of a tip vortex on buffet excitation near $C_{R\max}$ for the unswept wing models, it would be expected that a similar effect would occur at an incidence corresponding to $C_{R\max}$ for the aspect-ratio-eight and -ten forward-swept wing models, but no such effect is evident. Figure 11 indicates that no clearly defined $C_{R\max}$ exists for either the aspect-ratio-eight or -ten forward-swept wing models. These two features are probably related, but the mechanism is not understood.

For the aspect-ratio-twelve forward-swept wing model near 30 deg incidence, the value of $\sqrt{nG(n)}$ is much higher than for the lower aspect-ratio forward-swept wing models at similar values of reduced frequency (Fig. 14). With reference to Fig. 13, it would seem that for this combination of sweep angle, incidence, and aspect ratio, the tip vortex is again significantly increasing the buffet excitation. For a slight increase in incidence (2 deg) the buffet excitation parameter is

sharply reduced, suggesting that the tip vortex has lifted from the wing upper surface. For incidences beyong 32 deg, the presence of a swept bubble was again evident and the value of $\sqrt{nG(n)}$ is about 0.003, although the data suggest that the value may increase with a further increase in incidence.

Aerodynamic Damping

There are few published measurements of aerodynamic damping in separated flow for structural modes as determined by means of a buffeting investigation. For the aspect-ratio-sixteen wing models used in this investigation, it was possible to establish the presence of, and make some quantitative statements with respect to the magnitude of, the aerodynamic damping for fully separated flows and for the case when the leading-edge separation reattaches to the suction surface at approximately 50% chord (α = 2 deg).

In accordance with the method outlined in Ref. 16, it was established that at 2 deg incidence, the structural damping was insensitive to normal force and wing-root strain for these experiments. Thus, a systematic increase in total damping with velocity will indicate the presence of aerodynamic damping. This is shown to be the case in Fig. 15 for both the steel and aluminum aspect-ratio-sixteen wing models. Also presented in the figure are two solid lines which represent the aerodynamic damping computed from

$$\zeta_a = (\rho VcF(n)/8\pi mf_0) \int_0^{b/2} \phi^2(y) \cdot dc_L/d\alpha(y) \cdot dy \qquad (3)$$

The computed results from linear aerodynamic theory are in reasonable agreement with the experimental data points. Linear aerodynamic theory is applied here to indicate that the experimental data trends are reasonable and its use is justified, based on the fact that at 2 deg incidence, the separation reattaches to the upper surface at about 50% chord. It should not be inferred that the computed values represent the "exact" values of aerodynamic damping. The difference between the measured total damping and the computed aerodynamic damping is indicative of wind-on structural damping. The results suggest levels of wind-on structural damping of roughly 1% for the aluminum wing model and about 0.5% for the steel wing model. Equation (3) is based on the expression for aerodynamic damping found in Ref. 17, and modified to incorporate the variation in lift-curve slope across the span using lifting-line theory. The lift-curve slope had been determined in a separate experiment for a two-dimensional airfoil with the same section.[9] The effect of frequency on the lift-curve slope was accounted for using the Theodorsen function, $F(n)$.[18]

Further evidence of the presence of aerodynamic damping can be obtained from close examination of Fig. 16, wherein the variation in total damping is plotted against angle of incidence for the aspect-ratio-sixteen aluminum wing model. Two data points are shown at each incidence, reflecting the fact that this particular wind-tunnel run was repeated (several months after the initial test). As discussed in Ref. 9, experimental conditions are again such that the wind-on structural damping was constant over the incidence range 8 deg $\leq \alpha \leq$ 18 deg. The presence of aerodynamic damping remains to be established.

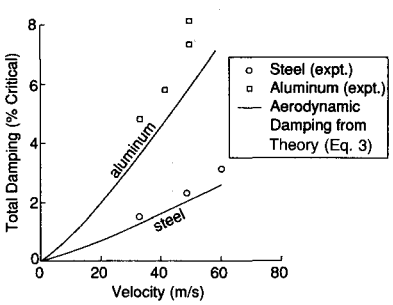

Fig. 15 Variation in total damping with velocity, AR = 16, Λ = 0 deg, α = 2 deg.

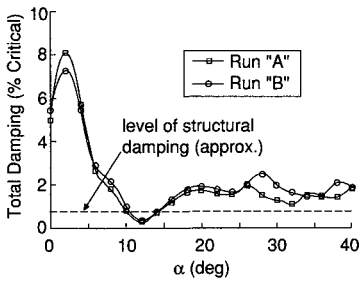

Fig. 16 Variation in total damping with incidence, AR = 16, Λ = 0 deg, V = 50 m/s.

With reference to Fig. 2, there is no appreciable slope to the curve of mean root bending-moment coefficient for incidences of 10 and 14 deg and it is reasonable to assume that the lift-curve slope would also be close to zero at these incidences. This implies that aerodynamic damping is not present, and therefore the total damping must be equivalent to the wind-on structural damping (indicated in Fig. 16). This level of structural damping is in reasonable agreement with the value of 1% suggested above. Indications of relative magnitudes of aerodynamic damping can be gleaned from the slope of the curve in Fig. 2 for the aspect-ratio-sixteen wing model. A steeper gradient indicates a larger magnitude of aerodynamic damping. Clearly, the aerodynamic damping should be positive at 8, 16, and 18 deg incidence. Furthermore, the magnitude of aerodynamic damping should be greater at 8 deg than at 18 deg and that at 18 deg should be greater than that at 16 deg. By similar argument, the aerodynamic damping should be negative at 12 deg. With reference to Fig. 16, at 12 deg incidence the total damping has decreased, and it can be concluded that the aerodynamic damping is negative. For incidences of 16, 18, and 8 deg, the total (and thus aerodynamic) damping is positive and increasing. Therefore, over the range 8 deg $\leq \alpha \leq$ 18 deg, it can be concluded that aerodynamic damping is present and that the aerodynamic and structural damping are of the same magnitude.

The structural damping of the aspect-ratio-sixteen aluminum wing model is roughly the same at an incidence of 2 deg and over the incidence range 8–18 deg. If it is assumed that this level of structural damping is present for the entire incidence range, then it can be said that for this wing model the aerodynamic damping represents a substantial contribution to the overall damping from 0 to 40 deg incidence (Fig. 16). Despite the fact that at some incidences there is a significant variation in the total damping, good agreement was obtained for the values of $\sqrt{nG(n)}$ for the two wind-tunnel runs.

Conclusions

This paper has discussed buffet excitation for wings in a low-speed flow. Measurements of the buffet excitation parameter were presented and discussed for a range of wing planforms, with an identical section chosen to be insensitive to Reynolds number effects. The following conclusions can be drawn from the results of the investigation.

1) The buffet excitation parameter $\sqrt{nG(n)}$ attains a value of 0.003 under poststall conditions and for reduced frequencies characteristic of aircraft in low-speed flight. Results from the unswept and aft-swept wing models indicated that $\sqrt{nG(n)}$ is insensitive to incidence under post-stall conditions; however, those from the forward swept models indicate that $\sqrt{nG(n)}$ may be sensitive to incidence. This level of excitation is attributed to that arising from a swept or unswept separation bubble, whichever is appropriate. The experimental evidence suggested that this limit is also valid for the second (overtone) bending mode.

2) Experimental evidence suggested that under certain conditions wing-tip vortices could influence the magnitude of $\sqrt{nG(n)}$ near stall. Levels in excess of the heavy buffet limit could be attained under these circumstances. Unsteady pressure measurements made under the tip vortex would confirm this source of buffet excitation.

3) Foci of separation are thought to cause excitation at reduced frequencies about an order of magnitude lower than those characteristic of wing buffeting in low-speed flight. It would therefore seem that foci are more of a concern for aircraft handling than for buffeting.

4) The insensitivity of the results to Reynolds number effects and the fixed separation point of the chosen section may provide a useful test case to determine $\sqrt{nG(n)}$ at high incidences using a CFD approach.

Acknowledgment

This research was financially supported by the Department of Trade and Industry (U.K.) under the technical direction of D. G. Mabey, RAE Bedford. S. J. Zan was on educational leave from the Institute for Aerospace Research for the duration of this investigation.

References

[1]Mabey, D. G. "Some Aspects of Aircraft Dynamic Loads Due to Flow Separation," AGARD R 750, Çeşme, Turkey, 1988.

[2]Mabey, D. G., and Chambers, J. R. "Unsteady Aerodynamics—Fundamentals and Applications to Aircraft Dynamics," AGARD AR 222, Göttingen, Germany, 1985.

[3]Winklemann, A. E., and Barlow, J. B. "Flowfield Model for a Rectangular Planform Wing Beyond Stall," *AIAA Journal*, Vol. 18, No. 8, Aug. 1980, pp. 1006–1008.

[4]Mabey, D. G., and Cripps, B. E. "Some Measurements of Buffeting on a Flutter Model of a Typical Strike Aircraft," *Ground/Flight Test Techniques and Correlation Conference*, AGARD CP 339, Paper 13, Çeşme, Turkey, 1983, pp. 13-1–13-16.

[5]Peake, D. J., and Tobak, M. "Three-Dimensional Interactions and Vortical Flows with Emphasis on High Speeds," NASA TM 81169, March 1980; see also AGARD AG 252, July 1980.

[6]Zingel, H. "On the Prediction of the Aeroelastic Behavior of Lifting Systems Due to Flow Separation," DFVLR Inst. for Aeroelasticity, European Space Agency Technical Translation 1043, Göettingen, Germany, Sept. 1987.

[7]Mabey, D. G. "Analysis and Correlation of Data on Pressure Fluctuations in Separated Flow," *Journal of Aircraft*, Vol. 9, No. 5, 1972, pp. 642–645.

[8]Hwang, C., and Pi, W. S. "Investigation of Northrop F-5A Wing Buffet Intensity in Transonic Flight," NASA CR 2484, Nov. 1974.

[9]Zan, S. J. "An Investigation of Low-Speed Wing Buffet," Ph.D. Dissertation, Univ. of Cambridge, Cambridge, England, UK, July 1990.

[10]Jones, J. G. "A Survey of the Dynamic Analysis of Buffeting and Related Phenomena," Royal Aircraft Establishment, TR-72197, Farnborough, England, UK, Feb. 1973.

[11]Coe, C. F., and Cunningham, A. M., Jr. "Predictions of F-111 TACT Aircraft Buffet Response and Correlations of Fluctuating Pressures Measured on Aluminum and Steel Models and the Aircraft," NASA CR 4069, May 1987.

[12]Cole, H. A., Jr. "On-Line Failure Detection and Damping Measurement of Aerospace Structures by Randomdec Signatures," NASA CR 2205, March 1973.

[13]Wick, B. H. "Study of the Subsonic Forces and Moments on an Inclined Plate of Infinite Span," NACA TN 3221, Ames, CA, June 1954.

[14]ESDU "An Introduction to Aircraft Buffet and Buffeting," Engineering Sciences Data Unit, Data Item 87012, London, July 1987.

[15]Zan, S. J., and Maull, D. J. "An Investigation of the Buffet Excitation Parameter," *Canadian Aeronautics and Space Journal*, Vol. 37, No. 2, June 1991.

[16]Mabey, D. G., and Butler, G. F. "Measurements of Buffeting on Two 65° Delta Wings of Different Materials," Royal Aircraft Establishment, Farnborough, England, UK, TR-76009, Jan. 1976.

[17]Williams, D. *An Introduction to the Theory of Aircraft Structures*, Edward Arnold Publishers, London, 1960, p. 364.

[18]Theodorsen, T. "General Theory of Aerodynamic Instability and the Mechanism of Flutter," NACA Rept. 496, Langley, VA, 1935.